Ramazan Asmatulu. Int. Journal of Engineering Research and Application www.ijera.com
ISSN : 2248-9622, Vol. 6, Issue 6, (Part -3) June 2016, pp.23-36

RESEARCH ARTICLE OPEN ACCESS

Enhanced Anti-Weathering of Nanocomposite Coatings with Silanized Graphene Nanomaterials

Ramazan Asmatulu,[a]*DaoudaDiouf,[a]Md.Moniruddin,[b]*and* Nurxat Nuraje[b]*
[a]*Department of Mechanical Engineering, Wichita State University, 1845 Fairmount, Wichita, KS 67260-0133*
[b]*Department of Chemical Engineering, Texas Tech University, P.O. Box 43121, Lubbock, TX 79409*

ABSTRACT

This article presents the development of a nanocomposite coating using nanographene platelets associated with an epoxy primer to improve the coating resistance against corrosion and weathering. Based on the hypothesis that coatings containing nanoadditives would provide strong resistance to degradation and that modified graphene particles through silanization improve the stability of the graphene particles in the coatings, the performance of the nanocomposite coatings was assessed by exposing them to ultraviolet (UV) light and salt fog by placing specimens alternatively in two respective chambers for intervals of 24 hours for 20 days. Coating performance analyses were carried out using atomic force microscopy (AFM), Fourier transform infrared (FTIR) spectrometer thickness measurements, water contact angle, and electro impedance spectroscopy (EIS) testing. Results show that a 17.15% reduction in coating thickness is observed for the coating containing silanized graphene in contrast to a 20.60% reduction in thickness for the coating with unmodified graphene. Furthermore, nanocomposite coatings containing unmodified graphene had a higher corrosion rate (38.71E-06 mpy) and a lower impedance value (75,040 ohms) than nanocomposite coatings containing silanized graphene, boasting a corrosion rate of 12.11E-06 mpy and an impedance value of 140,000 ohms, which confirmed the positive effects of graphene silanization.

Keywords: Graphene; Nanocomposite Coating; Composite Surface; UV Degradation; Prevention.

I. INTRODUCTION

Protective coatings are applied to surfaces in order to prevent deterioration in aircraft, sporting goods, automobiles, and marine applications.[1]They must satisfy the following requirements: retain a product‘s integrity facing environmental factors over a long period of time, (b) efficiently avert the absorption of moisture, (c) prevent the freeing of any toxic agents or side-products during a product‘s service life, and (d) be low in cost. Most protective coatings used in such cases are based on polyurethane (PU)-based compounds due to their outstanding properties, such as high tensile strength, chemical and weathering resistance, good processability, and mechanical properties.[2-4] However, polymeric material belongs to the organic coating family and generally deteriotes when exposed to environmental conditions. The degradation mechanism of PU has been studied for many years.[2,5-11]Briefly, degradation can occur when the amount of energy absorbed exceeds the bond energy of a polymer. The main factors contributing to environmental degradation include ultraviolet (UV) light, water, and oxygen.8,[12-22] Under UV irradiation, the chemical structure of materials irreversibly changes, which simultaneuosly affects both the physical properties—loss of gloss, yellowing, blistering, cracking, etc.—and mechanical properties—loss of tensile strength, brittleness, changes in glass transition temperature (Tg), etc.1 According to the principle of degradation,[5,23]ultraviolet light activates scissions of the urethane group, and the existence of the O_2 leads to the oxidation of the CH_2 group, which in turn leads to the formation of peroxide, ketone, and carbonyl near the polymeric coating surface. The oxidation by-products then get absorbed in the coating in wet environments and are unable to escape in dry environments, thus leading to adsorption. Water molecules also accelerate this process.

In order to improve the weathering problems of polyurethane coatings, in most cases, various UV absorbers and stabilizing agents are applied to minimize the absorption of UV light on the surface of the polymer by quenching free radicals or by absorbing high-energy radiation.[8,24-29] Furthermore, UV screeners[30] are inserted into the bulk polymer. UV radiation with energy ranging from 300 kJ/mol to 450 kJ/mol is considered to trigger major degenerative mechanisms for polymer coatings.[31] However, UV screeners are costly and degrade because of heavy UV exposure.[8,25,26,32]

The insertion of nanoparticles into polymeric coatings is one of the most promising methods to improve both their mechanical and weathering properties.[27,28] The nanoparticles used in coatings are SiO_2,[24,27] TiO_2,[28,33,34]ZnO,[30]

Al_2O_3,[35] and ZnS.[29] The selection of nanoparticles is based on the inherent properties they possess. Some nanomaterial additives that can be added to coatings for UV protection include ZnO and TiO_2.[36] Although they improve the anti-weathering properties of the coatings, anatasetitania nanomaterials produce free radicals due to their photocatalytic properties. Recently, Mirabedini et al.[34] studied the weathering performance of polyurethane nanocomposite coatings by suppressing the photocatalytic activity of titania modified with silane molecules. The incorporation of ZrO_2 nanoparticles into polymer coatings was reported to improve tribological characteristics, including reduced frictional coefficients and wear rates.[37] Nanocomposite coatings made of silica and polyamide exhibited higher scratch resistance than those without silica nanoparticles.[38] One study[39] shows the important relationship between microstructural details and tribiological properties of polymer nanocomposites. As the microstructural homogeneity of nanocompoistes was enhanced, their wear resistance was improved significantly.

However, to improve the anti-corrosion properties and mechanical properties of polyurethane, it is important to consider the intrinsic properties of the nanomaterials and design a water-repelling surface in order to prevent the acceleration of the weathering process with the influence of water. Therefore, polyurethane nanocomposite coatings with the addition of graphene nanoflakes have been developed by our research team.[40] Since graphene is a hydrophobic material that absorbs most of the incident light and has extraordinary mechanical strength (tensile strength between 0.5 and 1.0 terapascal),[41-44] it shows excellent potential to slow down the degradation process of coatings from environmental influences, such as water, UV light, and oxygen.

Our recent work[45] has proven that the insertion of graphene in polymer film increases water-repellency.[42] Therefore, based on our hypothesis, the weathering process can be prevented and/or retarded by using graphene since it absorbs incident light, provides mechanical durability, and increases hydrophobicity of the top coating. Graphene sheets in agglomerate form need to be properly dispersed in the coating to improve its corrosion and mechanical properties. These aggregations can be deterred by the attachment of other small polymers or molecules to the graphene sheet's surface, which is called silanization. The silanization process consists of covering the graphene surface with organofunctionalalkoxysilane molecules. A silane-type surfactant was applied to treat graphene nanoparticles (GNPs) in order to improve dispersion and interfacial bonding.

In this study, it is hypothesized that the inclusion of silanized graphene particles into polymer coatings improves their resistance to UV light and salt fog degradation to a greater extent than a coating containing inclusions of unmodified graphene.

The coating system employed on both a glass fiber-reinforced plastic (GFRP) and an aluminum alloy (AL 2024-T3) representing composite substrates and metallic substrates, respectively, generally consists of two layers: an epoxy-based primer and a polyurethane-based top coat, as shown in **Figure 1**. The specimens used as substrates were first coated with a base primer. Next, top coats containing the nanoadditives in different weight percentages were applied. The specimens were degraded by exposing them to two different experimental conditions: a weather test using a QUV accelerated weathering tester, and a corrosion using a Singleton salt spray chamber. Electro impedance spectroscopy (EIS) was used to evaluate the different levels of degradation seen on the control samples (0% silanized graphene [s-GNP]) versus samples with nanoadditives (2% s-GNP). After exposure, the surface morphology and chemical structure of the coatings were investigated with atomic force microscopy (AFM), scanning electron microscopy (SEM), and Fourier transform infrared (FTIR) imaging.

II. EXPERIMENTAL

2.1. Materials

Both glass fiber-reinforced composite (GFRC) (2.5 x 5.0 cm in size) and specific aluminum alloy (AL 2024-T3) specimens obtained from the National Institute for Aviation Research (NIAR) machine shop were used as substrates for coatings. AL 2024-T3 was chosen because it is primarily used in the manufacture of aircraft components. Aluminum alloy sheets (1 x 2 in) were coated with the nanocomposite for EIS testing. Sherwin Williams CM0482300 epoxy primer together with Sherwin Williams CM0120900 epoxy adduct, which is a polyamine-based compound that works as a hardener in conjunction with CM0482300, was painted on the composites asthe base coat. Jet Glo® CM0570535 570 series Matterhorn White, a polyester urethane-based compound that shows excellent bonding with epoxy primers, along with the Jet Glo® hardener CM0578520, was used as the top coat. Nanosize graphene platelets were purchased from Angstron (product number N008-100-N). At least 80% of the graphene platelets had a Z-dimension of <100 nm. A Fisher Scientific FS 200 sonicatorwas used to assist with breaking up the agglomeration of the nanoparticles to ensure uniform distribution of the nanoadditives. [3- (2-Aminoethylamino) propy] trimethoxysilane was purchased from Sigma-Aldrich, Inc.

2.2. Methods

2.2.1. Silanized Graphene (s-GNP) Preparation

Organosilane ([3- (2-Aminoethylamino) propy] trimethoxysilane) was used to silanize pristine graphene according to the work of Li et al.[46] In this preparation, 2 grams of pristine graphene was dispersed in 200 ml ethanol (95%) by high power ultrasonication for one hour. The flask was then heated up to approximately 120°C to boil the ethanol under magnetic stirring. Then 12 ml of the silane surfactant was added drop-wise into the sealed Erlenmeyer flask. After five hours of reaction, the graphene/ethanol mixture was cooled down to room temperature, and the resulting silanized graphene suspension was rinsed with 500 ml deionized (DI) water using a filtration process. The silanized graphene was then dried overnight in the oven at 70°C for further use.

2.2.2. Preparation of Substrates

To ensure good bonding between the GFRC or aluminum, and the coating, the surfaces of either substrate were sanded using 3M 413Q abrasive sandpaper with a 400 grit number. Then the surfaces were cleaned with DI water and acetone.

2.2.3. Preparation of Base Coat

The base coat was prepared by mixing the CM0482300 epoxy primer with the CM0120900 epoxy adduct in a 1:1 weight ratio. Then the mixture was stirred slowly for 15 minutes before being used on the test samples. The nanocomposite base coat was developed by adding silanized graphene to the standard base coat in 2%, 4%, and 8% weight percentages. In this preparation, first the nanoadditives were added into the epoxy adduct, and then the mixture was placed in a sonicator at room temperature for 30 minutes. After 30 minutes of sonication, the epoxy adduct was added to the epoxy primer and magnetically stirred on a hot plate for four hours at room temperature, which allowed a good distribution of nanoadditives in the base coat.

2.2.4. Preparation of Top Coat

Graphene nanoflakes or silanizedgraphenes were mixed well with the polyester urethane top coat via 30 minutes of probe sonication followed by four hours of high-speed mechanical agitation. The basic top coat consisted of mixing the Jet Glo® white paint with the Jet Glo® hardener in a 1:1 ratio by weight. Then the mixture was stirred slowly for 30 minutes before being used on the test samples. A series of nanocomposite top coats were respectively prepared by adding silanized graphene with 2%, 4%, and 8% weight percentages. In this preparation, first the nanoadditives were added into the Jet Glo® hardener, and then the mixture was placed in a sonicator at room temperature for 30 minutes. After 30 minutes of sonication, the Jet Glo® hardener was added to the Jet Glo® white paint and magnetically stirred on a hot plate for four hours at room temperature. To ensure uniform testing conditions and maintain uniform coating of 2 mils (50.8 microns) on all test specimens, the thickness of the coating was measured using a Mitutoyo 293-725 digital micrometer.

2.2.5. UV Exposure Test

The UV degradation test was performed using the QUV accelerated weathering chamber, purchased from the Q-Panel Company. Tests were in compliance with SAE standard ASTM D 4587-09, which describes the basic process of exposing paint and related coatings to UV light. The specimens were tested for a total of 20 days and characterized for surface morphology, hydrophilic/hydrophobic behavior, and also coating thickness in four-day intervals.

2.2.6. Corrosion Test

The corrosion test was performed in a Singleton salt spray chamber according to SAE standard ASTM B117, which describes the procedure of corrosion testing after exposure to the UV-condensation test. Specimens were put in the corrosion chamber on racks with slots at a 15-degree angle. The pH was kept between 6.7 and 7.2, and the fog concentration averaged 1.2 ml/hour, as suggested by the testing standard. Specimens were alternatively maintained inside the corrosion chamber and the UV chamber in 24-hour intervals for a period of 20 days.

In order to study the degradation mechanism of the polyurethane coating, an attenuated total reflectance (ATR) FTIR study of the test samples was conducted before and after UV exposure using a Thermo Nicolet Magna 850 IR spectrometer. The surface properties of the films were investigated via an optical water contact angle goniometer (Model CAM 100), which was purchased from KSV Instruments Limited. Atomic force microscopy was used to image the surfaces of the coating before and after UV and corrosion exposure. An MFP-3D-SA stand-alone atomic force microscope purchased from Asylum Research was used in our characterization process.

2.2.7. Electro Impedance Spectroscopy

EIS was applied to study the different levels of degradation of the control sample (0% s-GNP) and nanocomposite sample (2% s-GNP) prepared on aluminum substrates. Potentiostatic and potentiodynamic testing of bare samples, control samples, and samples containing 2% silanized graphene were performed using the Gamry Reference 600 potentiostat in a 0.5 molNaCl solution.

2.3 Application of Coatings

Coatings were fabricated using the Preval® spray system. The required times for production of a thickness of 2.0 to 3.0 mils of dry film is between 16 and 18 hours for unaccelerated drying and between 2 and 3 hours for accelerated drying. The glass fiber-reinforced plastic or aluminum specimens were first coated with a base primer and then applied with a top coat once the base primer had cured.

III. RESULTS AND DISCUSSION

A series of coatings containing silanized graphene with 2%, 4%, and 8% weight percentages on the glass fiber-reinforced plastic or aluminum specimens were fabricated using the Preval® spray gun. In this fabrication, the GFRP or aluminum specimens were first coated with the base primer. Then, top coats were spray coated onto the composite samples. The spray process was controlled to limit the thickness of the coating to 1 mils (25.4 microns). The total thickness of the coating system (base primer + top coat) was 2 mils (50.8 microns). To mimick natural weathering conditions, including sunlight and rain or dew, all samples were tested in the UV chamber and salt-corrosion chamber.

An alternating cycle between absorption and adsorption under climate conditions causes deterioration of polymer coatings; once deterioration of polyurethane begins, the formation of cracks and blisters take place. The increased formation of cracks and blisters due to continued exposure leads to the release of pigment cells, and their reduction results in a small reduction of the coating thickness. During the period of testing, it was found that polymer coatings with and without silanized graphene experienced a reduction in thickness, which is because of the compaction of coating under UV light, and oxide layer formations followed by erosion in the corrosive environment [47,48].

For coatings not containing the inclusion of silanized graphene, the original coating thickness was 2.12 mils before UV and corrosion exposure; however, after 20 days of alternative UV and salt fog exposure, the thickness decreased to 1.67 mils, a 26.95% decrease in coating thickness, as shown in **Figure 1**. For the coatings containing 2% silanized graphene particles, the original coating thickness was also 2.12 mils before UV and corrosion exposure, but after the same period of climate condition treatment, the thickness decreased to 1.81 mils, a 17.13% decrease in coating thickness. **Figure 1** shows even better results with the decrease in coating thickness of 10.78% and 8.72% for those coatings with 4% and 8% silanizedgraphenes, respectively. It can be concluded from these results that nanocomposite coatings with an increased percentage of silanized graphene have improved resistance to UV and salt fog degradation, which is depicted by a lesser decrease in coating thickness. Also, this is consistent with our previous study, which showed that the inclusion of unmodified graphene particles into a polymeric coating leads to a decreased reduction in coating thickness after UV and salt fog exposure[40]; however, after 20 days of climate condition treatment, a 20.60% reduction in the coating thickness is noticed for the polyureathane coating with unmodified graphene, while in this study, only a 17.13% reduction in coating thickness is observed forpolyureathane coating modified with silanized graphene. This is an indication that silanized graphene improves the resistance of polymer coating to degradation to a greater extent than unmodified graphene.

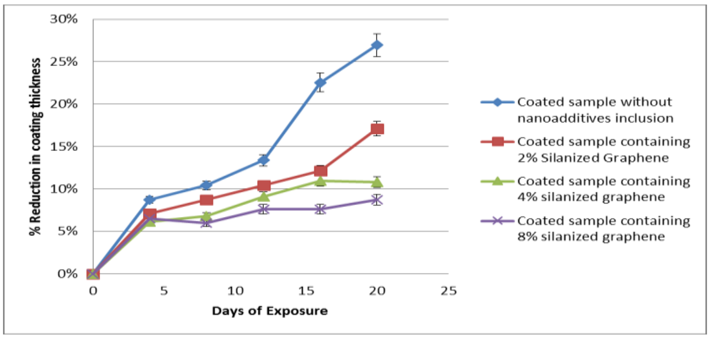

Figure 1: Percentage Thickness Reduction of Various UV and Salt Fog Exposed Samples Containing Different Percentages of Nanoadditives. The bar is plus/ minus 0.2 mil.

It can be observed that coated test samples containing 2% silanized graphene particles have greater resistance to degradation than coated test samples without nanoadditive inclusions. In addition, it can be seen that an increased percentage of silanized graphene particlesup to 8% leads to greater resistance to UV and salt fog degradation. Also, an additional study comparing samples containing silanized graphene with unmodified graphene showed there is an exponential decrease in coating thickness for coated samples containing 2% unmodified graphene, while for a nanocomposite coating containing silanized graphene, the decrease in coating thickness is steadier. The improved performance of nanocomposite coatings with silanized graphene could be due to the fact that one of the functions of silanization is to help in the dispersion of graphene in polymer coatings or other media and thus inhibits the aggregation of graphene sheets throughout the coating. The reduced number of graphene aggregates inside the coating could lead to less stress points from which crack formation could start and hence lead to a diminished reduction in coating thickness.

For a comparison of coatings with and without the addition of silanized graphene, we chose two samples with which to do weathering experiments. Here, two samples were alternatively incubated for 20 days in both UV and salt fog chambers. One sample was with the polyureathane coating only. The other sample was the coating with the addition of 2% silanized graphene nanomaterials.

The coatings were studied under a microscope to observe their topographical changes before and after weathering experiments. **Figure 2(A)** shows an AFM image of the surface of a coated test sample containing 0% silanized graphene particles before exposure to UV light or the salt fog test. The reduced presence of surface roughness of the specimen indicates significant gloss. But after 20 days of UV light and salt fog exposure. The surface of the coating was completely ruined, and the formation of blisters of various sizes can be clearly seen in **Figure 2(C)**. In addition to blistering, which is the most obvious indication of UV degradation, a strong presence of small cracks can be seen over the entire sample's surface.The combination of blistering and crack formation on the surface of the sample indicates the degradation of the coating after 20 days of UV and salt fog exposure. **Figure 2(B)**shows an AFM image of the surface of a coated test sample containing 2% silanized graphene particles that has not been exposed to UV or corrosion tests. Due to the presence of silanized graphene nanomaterials, the surface of the sample is rougher, showing dispersion of graphene nanoparticles inside the polymer coatings. Likewise, the inclusion of nanoparticles on the surface of the coating, was also confirmed by SEM images (**Figure 3**), which show good dispersion of the silanized graphene inside the coating. **Figure 2(D)** isan AFM image of the coating sample containing 2% silanized graphene after 20 days of UV and salt fog exposure. In this case, no blistering is visible on the surface of the coated test specimen. Consequently, the nanocomposite coating containing 2% silanized graphene ought to offer improved corrosion resistance.

However, we do notice crack formation on the surface of the coating. This crack formation is likely the result of severe corrosion / degradation and is often seen on conventionally used polymeric coatings. In some cases, crack formation can also be due to increased brittleness of the coated sample because of the inclusion of nanoparticles. It has been proven that the agglomeration rate of a nanoparticle increases as a function of its inclusion in a polymer coating. But due to the lack of changes seen on the surface of the 2% s-GNP nanocomposite coating, these AFM images strongly suggest that the resistance to degradation of a nanocomposite coating containing silanized graphene is much better than for a coating devoid of nanoparticle inclusion.A previous study of Nuraje et al. showed that even a coating containing 2% unmodified graphene displayed significant amounts of degradation after 20 days of UV and salt fog exposure; the changes were depicted by the formation of cracks, pits, and blisters.[40] However, in the case of a nanocomposite coating containing silanizednanoadditives (2% s-GNP), only crack formation is seen on the surface of the sample, suggesting the superiority of nanocomposite coatings containing silanized graphene over nanocomposite coatings containing unmodified graphene.

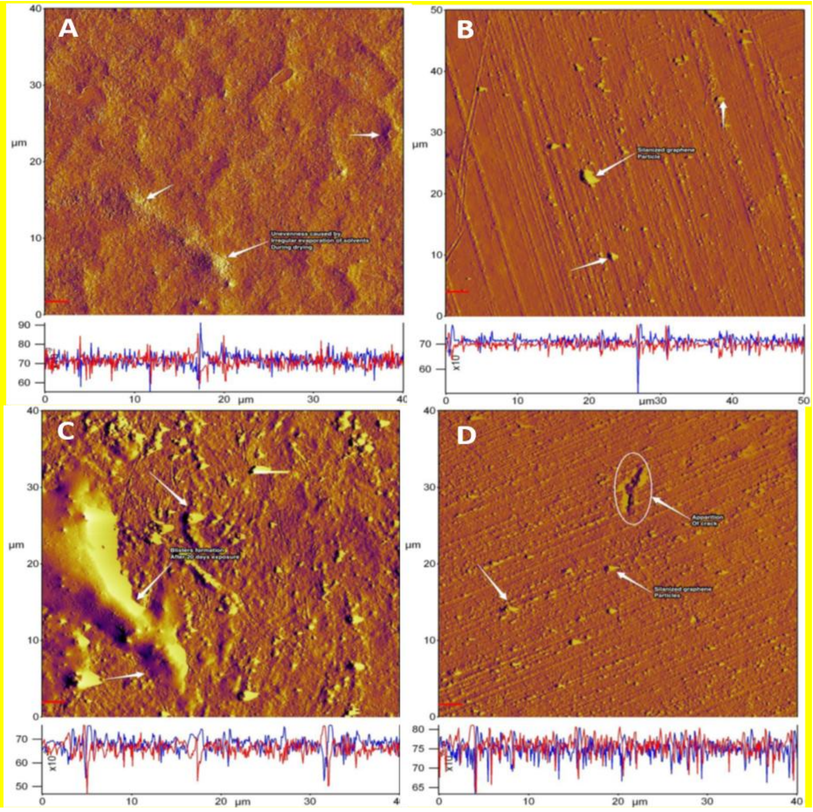

Figure 2. AFM AmplitudeImageofPolureathane Coatings: (A)with Addition of 0% Silanized Graphene, (B) with addition of 2% Silanized Graphene, (C) After UV and Salt Fog Exposure and Polyureathane coatings with 0% Silanized Graphene, and (D) with 2% Silanized Graphene after UV and Salt Fog Exposure.

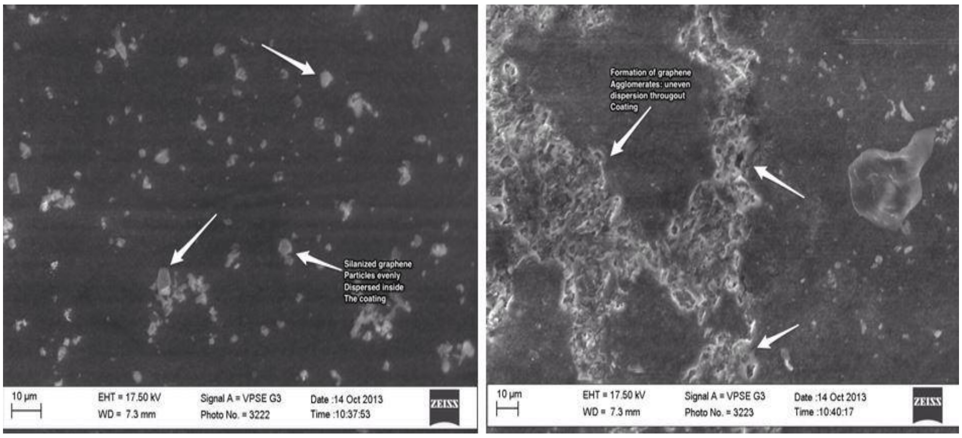

Figure 3. SEM Images of Nanocomposite Coating Containing Silanized Graphene (left) and Unmodified Graphene (right).

Before UV and salt degradation, the shininess and smoothness of the sample leads to higher contact angle measurements. The contact angle change of the above coatings were investigated using a goniometer. In the absence of a protective coating, a rapid decrease in contact angle values after 20 days' exposure was observed with the time series degradation of bare glass fiber composite samples, which was from 65.23° to 37.31° after 20 days exposure. The time series degradation of the contact angle of bare glass fiber composite specimens coated with a polymer coating but without nanoadditives varied from 69.66° to 46.85°, which is better than for the bare glass fiber specimens. However, the time series degradation of the contact angle of bare glass fiber composite specimens coated with a polymer coating containing 2% silanized graphene varied from 78.85° to 50.89° after UV and salt exposure, which represents an improvement over the basic coating.

For bare glass fiber composite specimens coated with a polymer coating containing 4% silanized graphene, the contact angle values varied from 80.45^o to 52.99 ^{o} after UV and salt fog exposure, which was a better performance than the coating containing 2% silanized graphene. The time series degradation of the contact angle for a polymer coating containing 8% silanized graphene was from 81.23^o to 54.7 ^{o} after UV and salt fog exposure. This sample displayed the most resistance to UV and salt fog degradation. The contact angles seen in this case were consistently higher than for coatings with 2%, 4%, and 8% silanized graphene. The higher percentage of silanized graphene did not affect the properties of the coating, while in the case of 8% unmodified graphene inclusion, the coating was susceptible to deterioration.

Overall, AFM served as a good visual indicator of the degradation process. Two conclusions can be drawn from the AFM images. First, a nanoadditive-like graphene, when added to a coating, can act like a reinforcement that binds the pigment cells and increases the resistance of the coating against environmental factors, such as UV degradation and corrosion. Graphene absorbs all of the light and provides hydrophobicity. Second, the mechanism of coating degradation, which proceeds through the formation of blisters, pits, and cracks on the surface, resulting in the loss of coating properties, has been reestablished.

To understand the mechanism of UV and corrosion damage to the coatings, ATR-FTIR imaging was applied to further investigate any changes at the molecular level. The aim of carrying out the FTIR studies was to test the hypothesis that the degradation of the PU coatings may occur due to UV exposure by the formation of certain types of compounds, such as carbonyl, aldehydes, ketones, and peroxide groups, as the result of scission of chains in the polyurethane. The FTIR spectrum (**Figure 4**) shows some changes in the properties of a polyurethane coating as a function of UV exposure. **Figure 4(A)** shows the ATR-FTIR spectrum of a test sample containing 0% silanized graphene, displaying various peaks that indicate the loss of breakage of chemical structures due to exposure to UV light or the formation of chemical structures. From the **Figure 4(A)** spectrum, it can be learned that a first peak characteristic of the stretching of N-H group at 3125 cm-1 implies the formation of polyuria.[6] The small peak seen at 2,130 cm^{-1} suggests the symmetric and asymmetric stretching of the CH_2 group, while the vibrations signals seen between 2200 and 1900 cm^{-1} is an indication of the vibration and stretching of the C=O bond. The five peaks shown at 2181.20, 2144.46, 2029.49, 1992.10, and 1976.58 cm-1 suggest that the C=O bond is stretching further, and a clear sign of the presence of polyurea is the distinct peak seen at 1505.63cm^{-1}. Another peak at 1035.92 cm^{-1} suggests a diminution of the C-H group, while a peak at 826.32 cm^{-1} shows reduction in the C-O group. Another peak is noticed at 555.71 cm^{-1}, showing the establishment of the ester group, and a chain scission of the polyurethane is indicated by the decrease of the C-O and C-H group. **Figure 4(B)** shows the ATR-FTIR spectrum of a test sample containing 2% silanized graphene. The peak seen at 2955.74 cm^{-1} shows the existence of polyuria, while small vibration signals between 2200 and 1800 cm-1 suggest vibration of the C=O bond; after this vibration signal, an array of peaks at 1700, 1456.12, 1243.69, and 1170 cm^{-1} all hint at the presence of polyurea. The small peak at 450 cm^{-1} suggests a reduction in the C-O group, but the decreased ratio of peaks after 1500 cm^{-1} suggests a limited development of ester in this particular coated test sample; this reduction in the number of peaks could be due to the inclusion of silanized graphene inside the coating.

The silanized graphene could be acting as an absorbing agent for the UV radiation and hence contributing to a reduced development of ester in the coating. To confirm this hypothesis, an additional FTIR spectrum of a test specimen containing a higher percentage (4%) of silanized graphene by weight was taken. **Figure 4(C)** shows the ATR-FTIR spectrum of a coated test sample containing 4% silanized graphene, which displays UV degradation to an even lesser extent than the coated test sample containing 0% silanized graphene and 2% silanized graphene. The peak seen at 2923.73 cm^{-1} shows the existence of polyurea due to the stretching of the NH bond; as in previous cases, the vibration signals between 2400 and 1900 cm^{-1} suggest vibration of the C=O bond. After this vibration signal, there are two clear peaks at 1445.29 and 902.26 cm^{-1}, all hinting at the presence of polyurea. However, a clear reduction in peaks after 1500 cm^{-1} suggests that there is not a reduction in the C-O group and that ester formation has been significantly reduced. Because ester formation is decreased as the percentage of silanized graphene is increased in the coating, it can be concluded that the silanized graphene acts as an agent that absorbs part of the UV radiation to which the polyurethane-coated test sample is exposed and hence reduces its degradation.

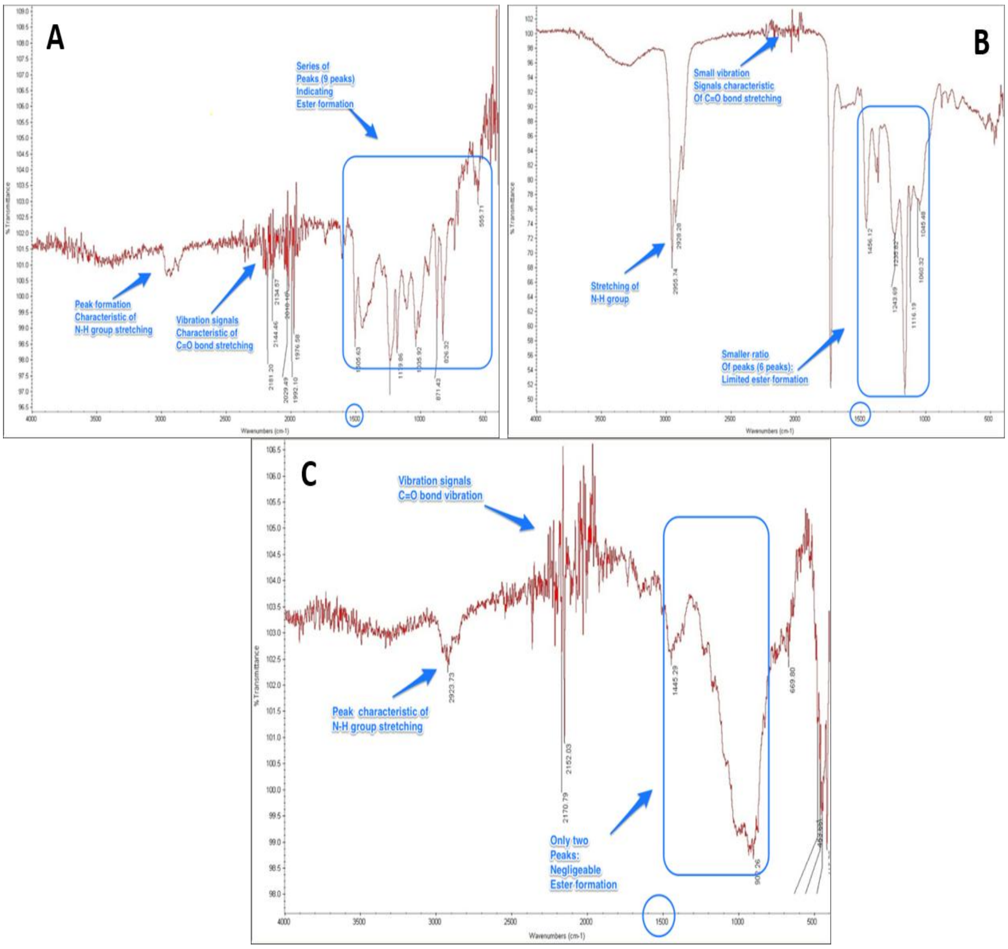

Figure 4. (A) ATR-FTIR Spectrum of Coated Test Sample with 0% Silanized Graphene, (B) 2% Silanized Graphene, and (C) 4% Silanized Graphene after 20 Days of UV + Salt Fog Exposure.

To confirm the improved performance of coatings containing silanized graphene compared to coatings with no nanoadditives in terms of corrosion protection, potentiostatic and potentiodynamic tests were performed on aluminum substrates. **Figure 5** depicts the comparative Tafel curves of nanocomposite coatings containing 8% silanized graphene (S5), 4% silanized graphene (S4), 2% silanized graphene (S3), coatings without nanoadditive inclusions (S2), and bare aluminum alloy AL 2024-T3 samples (S1). The corrosion potential is indicated by the intersection of the slopes of the cathodic and anodic branches of the curve. Potentiodynamic test values of all specimens are represented in **Table 1**. The bare aluminum sample has a corrosion rate of 420.1E-3 mpy (micrometers per year). For the aluminum sample coated with a coating containing 0% silanizedgraphene, the corrosion rate is 4.93E-03 mpy, but for the coated specimen containing 2% silanized graphene, the corrosion rate is 12.11E-06 mpy. The observed corrosion rates show that the test specimen containing 2% silanized graphene corroded at a slower rate than the coated test sample without nanoadditives. In addition, it was observed that an increased loading of silanized graphene by weight into the coating resulted in an improved resistance to corrosion; the sample containing 8% silanized graphene had the lowest corrosion rate of 3.115E-06. A our previous study[49] showed that coatings containing 2% unmodified graphene (S7) displayed an even greater resistance to corrosion, boasting a corrosion rate of only 4.52E-07 mpy; however, the samples were first treated with a corrosion-inhibiting tin alloy before being coated, which explains the observed high resistance to corrosion.

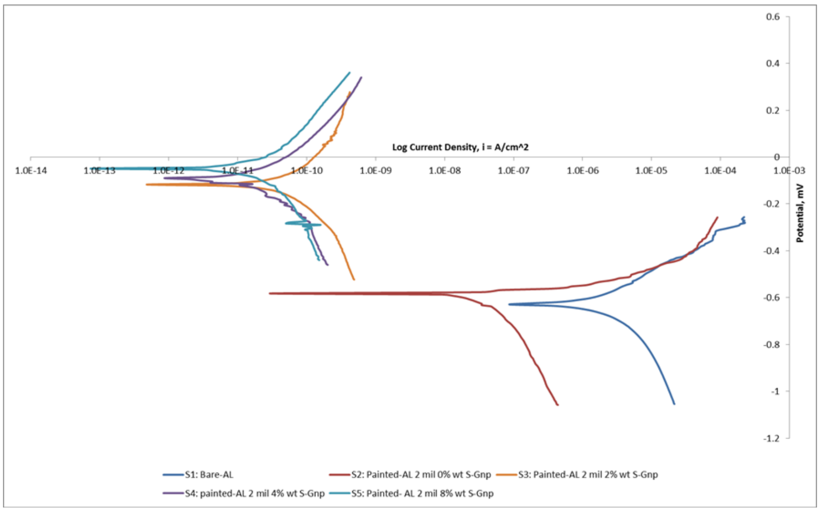

Figure 5 Tafel Curves of Various AL Samples Coated with Different Percentages of Nanoadditives.

Table 1 Corrosion Values Of Various Test Samples Containing Different Percentages OfNanoadditives By Weight

Code Names	**Sample Names**	**Icorr (A)**	**Ecorr (V)**	**Corrosion Rate (mpy)**
S1	Aluminum (bare)	4.750×10^{-12}	-0.628	420.1E-03
S2	Coating with primer 0wt% silanized graphene	5.57×10^{-8}	-0.585	4.930E-03
S3	Coating with primer 2wt% silanized graphene	1.37×10^{-10}	-0.120	12.11E-06
S4	Coating with primer 4wt% silanized graphene	5.48×10^{-11}	-0.0844	4.851E-06
S5	Coating with primer 8wt% silanized graphene	3.52×10^{-11}	-0.051	3.115E-06
S6	Coating with primer 2wt% unmodified graphene	4.37×10^{-10}	-0.119	38.71E-06
S7	Sn-Cu coating with primer 2wt% unmodified graphene	2.32×10^{-11}	-0.341	4.52E-07

A comparative study was conducted to see the difference between a test sample painted with a nanocomposite coating containing unmodified graphene versus a nanocomposite coating containing silanized graphene. The corrosion rate for the tested sample painted with a coating containing 2% unmodified graphene (S6) was 38.71E-06 mpy, while the corrosion rate of a nanocomposite coating containing silanizedgraphene (2% s-GNP) was only 12.11E-06 mpy, further confirming the superiority of the nanocomposite coatings containing silanized graphene over nanocomposite coatings containing unmodified graphene in terms of corrosion protection.

Figure 6 shows the difference in corrosion rates between a coating containing 2% silanized graphene and a coating containing 2% unmodified graphene.

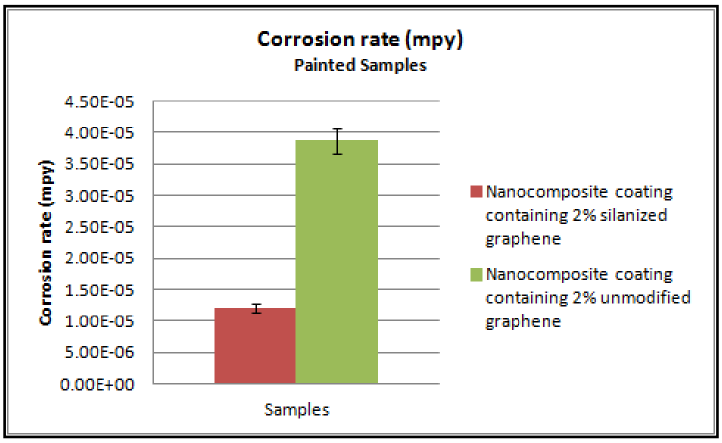

Figure 6. Corrosion Rate Comparison of Coated Test Samples Containing Unmodified Graphene Particles versus Coated Test Samples Containing Silanized Graphene Particles.

In addition to the potentiodynamic test which showed the corrosion rate of the test samples, a potentiostatic test was performed to determine the surface resistance of the test specimens. The potentiostatic test values of all specimens are displayed in **Table 2**. The bare aluminum sample has an impedance value of 14. 39 Ω (ohms). For the aluminum sample painted with a coating containing 0% silanized graphene, the impedance value is 36,350 Ω, but for the coated specimen containing 2% silanized graphene, the impedance value is 140,000 Ω. The observed impedance values showed that the test specimens containing 2% silanized graphene had a higher surface resistance than the coated test sample without any nanoadditive inclusions. However, it was shown that test samples[49] containing 2% unmodified graphene displayed an infinite impedance resistance when subjected to the same test; in that particular case, however, the aluminum substrate was treated with a chromate conversion coating designed to inhibit corrosion before the application of paint, while in this study our samples were untreated. This could be the reason for the higher impedance values obtained with nanocomposite coatings containing unmodified graphene. An infinite impedance value is obtained when the coating is unaltered, leading to a Nyquist plot represented by an almost vertical line, as shown in **Figure 7**. The various Nyquist plots shown in **Figure 7** are plotted on the same scale; however, because of the significant difference in impedance values between the samples, the bare aluminum sample is not seen in this figure.

Table 2 Impedance Resistance Of Various Test Samples Containing Different Percentages Of Nanoadditives By Weight

Code Name	**Sample Names**	**Impedance Resistance (□)**
S1	Aluminum (bare)	14.39
S2	Coating with primer 0wt% silanized graphene	36,350.00
S3	Coating with primer 2wt% silanized graphene	140,000.00
S4	Coating with primer 4wt% silanized graphene	165,400.00
S5	Coating with primer 8wt% silanized graphene	284,100.00
S6	Coating with primer 2wt% unmodified graphene	75,040.00
S7	Sn-Cu coating with primer 2wt% unmodified graphene	Infinite

The comparative study between a test sample painted with a nanocomposite coating containing unmodified graphene versus a nanocomposite coating containing silanized graphene showed that the impedance value for the test sample painted with a coating containing 2% unmodified graphene was 75,040 Ω, while in the case of a nanocomposite coating containing silanized graphene (2% s-GNP), the impedance resistance was 140,000 Ω.. These results suggest that silanized graphene improves the resistance of a nanocomposite coating to corrosion. **Figure 7** shows the difference in impedance resistance between a coating containing 2% silanized graphene and a coating containing 2% unmodified graphene.

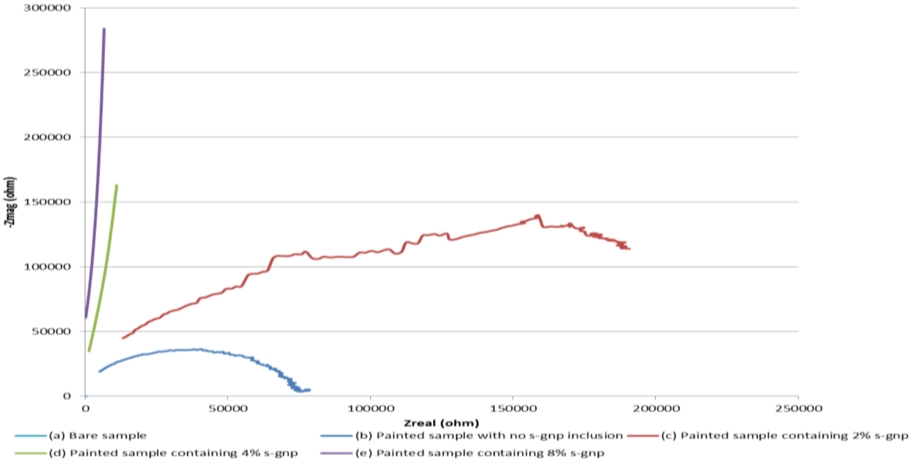

Figure 7: Nyquist Curves: (a) Bare Sample, (b) Painted Sample with No Inclusion, (c) Sample Painted with Coating Containing 2% Silanized Graphene, (d) Sample Painted with Coating Containing 4% Unmodified Graphene, (e) Sample Painted with Coating Containing 8% Silanized Graphene.

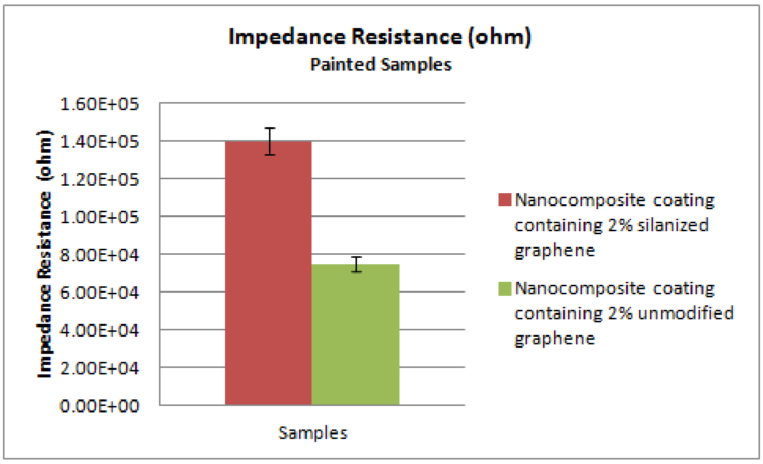

Figure 8: Impedance Resistance Comparison of Coated Test Samples Containing Unmodified Graphene Particles versus Coated Test Samples Containing Silanized Graphene Particles.

IV. CONCLUSIONS

Graphene in different weight percentages was added to polyurethane coatings, and subsequently tests were conducted to check the variation in properties of the coatings. Test samples were prepared by the addition of 0%, 2%, 4%, and 8% weight percentage of graphene into standard polyurethane coatings. FTIR spectroscopy, AFM examination, and water contact angle tests were performed to quantify the variation in properties. These tests confirmed the hypothesis that the addition of graphene does in fact improve the resistance against UV degradation and corrosion. The polyurethane coating containing 2% graphene showed greatly improved performance compared to the standard polyurethane coating, since graphene provides hydrophobicity, absorbs incident light, and improves mechanical robustness of the coatings. Also, the detailed FTIR analysis reinforced the hypothesis that degradation of polyurethane coatings occurred due to the formation of certain water soluble compounds, such as carbonyls, aldehydes, ketones, and peroxides. Through a time series study of the AFM images at different stages of the UV and corrosion tests, the progression of degradation was explained in detail by the formation and enlargement of blisters, pits, and cracks. Overall, this research has provided a detailed overview of the mechanism of coating degradation and has suggested a means to arrest or decrease the rate of this degradation by using a nanoadditive, namely graphene.

ACKNOWLEDGMENT

Authors would like to acknowledge Wichita State University for the technical support of this work.

REFERENCES

[1]. *Nanostructured thin films and nanodispersion strengthened coatings*1ed.; Springer: Netherlands, 2004.

[2]. Aglan, H., Calhoun, M., Allie, L. Effect of uv and hygrothermal aging on the mechanical performance of polyurethane elastomers. *Journal of Applied Polymer Science* 2008, *108*, 558-564.

[3]. Oertel, G., Abele, L. *Polyurethane handbook: Chemistry, raw materials, processing, application, properties*. Hanser: 1994.

[4]. Ramakrishna, S., Mayer, J., Wintermantel, E., Leong, K.W. Biomedical applications of polymer-composite materials: A review. *Composites Science and Technology* 2001, *61*, 1189-1224.

[5]. Yang, X.F., Tallman, D.E., Bierwagen, G.P., Croll, S.G., Rohlik, S. Blistering and degradation of polyurethane coatings under different accelerated weathering tests. *Polymer Degradation and Stability* 2002, *77*, 103-109.

[6]. Yang, X.F., Vang, C., Tallman, D.E., Bierwagen, G.P., Croll, S.G., Rohlik, S. Weathering degradation of a polyurethane coating. *Polymer Degradation and Stability* 2001, *74*, 341-351.

[7]. Ludwick, A., Aglan, H., Abdalla, M.O., Calhoun, M. Degradation behavior of an ultraviolet and hygrothermally aged polyurethane elastomer: Fourier transform infrared and differential scanning calorimetry studies. *Journal of Applied Polymer Science* 2008, *110*, 712-718.

[8]. Merlatti, C., Perrin, F.X., Aragon, E., Margaillan, A. Natural and artificial weathering characteristics of stabilized acrylic-urethane paints. *Polymer*

Degradation and Stability 2008, *93*, 896-903.

[9]. Pappas, S.P. Weathering of coatings - formulation and evaluation. *Progress in Organic Coatings* 1989, *17*, 107-114.

[10]. Fernando, B., Shi, X., Croll, S. Molecular relaxation phenomena during accelerated weathering of a polyurethane coating. *J Coat Technol Res* 2008, *5*, 1-9.

[11]. Bauer, D.R. Degradation of organic coatings. I. Hydrolysis of melamine formaldehyde/acrylic copolymer films. *Journal of Applied Polymer Science* 1982, *27*, 3651-3662.

[12]. SP, P. Weathering of coatings-formulation and evaluation. *Progress in Organic Coatings* 1989, *17*, 107.

[13]. W, S. *Polymer degradation, principles and practical applications.* Macmillan: New York, 1981.

[14]. Blakey. Evaluation of paint durability-natural and accelerated. *Progress in Organic Coatings* 1985, *13*, 279-296.

[15]. Bauer. Degradation of organic coatings: Hydrolysis of melamine formaldehyde/acrylic copolymer films. *J Appl Polym Science* 1982, *27*, 3651-3662.

[16]. Xiao GZ, S. Water absorption and desorption in an epoxy resin with degradation. *Journal of Polymer Science: Part B: Polymer Physics* 1997, *35*, 2659-2670.

[17]. Morrow AM, A.N., Edge M. Photodegradation of waterbased acrylic coatings containing silica. *Journal of CoatingsTechnology* 1988, *70*, 65-72.

[18]. Bauer. Network formation and degradation in urethane andmelamine-formaldehyde crosslinked coatings. . *American ChemicalSociety, Division of Polymeric Material Science and Engineering* 1987, *56*, 91-95.

[19]. Bauer. Melamine/ formaldehyde crosslinkers: Characterization,network formation and crosslink degradation. *Progress in Organic Coatings* 1986, *14*.

[20]. Bauer DR, D.R., Koenig JL. Cure in photogradation of 2- package acrylic/urethane coatings. *Industrial Engineering and Chemistry Product and Research Development* 1986, *25*.

[21]. Gerlock JL, V.O.H., Bauer DR. Nitroxide kinetics during photodegradation of acrylic/melamine coatings. *European Polymer Journal of Coatings* 1983, *19*, 11-18.

[22]. Lefebvre DR, T.K., Muller AJ, Raju VR. Degradation of epoxy coatings in humid environments: The critical relative humidity ofr adhesion loss. *Journal of Adhesion Science and Technology* 1991, *5*, 201-227.

[23]. Rånby, B.G., Rabek, J.F. *Photodegradation, photo-oxidation, and photostabilization of polymers: Principles and applications*. Wiley: 1975.

[24]. Jabbarnia, A., Khan, W.S., Ghazinezami, A. and Asmatulu, R. “Tuning the Ionic and Dielectric Properties of Electrospun PVdF/PVP Nanofibers with Carbon Black Nanoparticles for Supercapacitor Applications,” *International Journal of Engineering Research and Applications* (in press).

[25]. Decker, C., Masson, F., Schwalm, R. Weathering resistance of waterbased uv-cured polyurethane-acrylate coatings. *Polymer Degradation and Stability* 2004, *83*, 309-320.

[26]. Lee, B.-H., Kim, H.-J. Influence of isocyanate type of acrylated urethane oligomer and of additives on weathering of uv-cured films. *Polymer Degradation and Stability* 2006, *91*, 1025-1035.

[27]. Xiao,S., Yang, W., and Zhang, Y. “Studying Nanotube-based Oscillators and Their Application as Memory Cells via Nanoscale Continuum Modeling and Simulation,” *Int. Journal of Engineering Research and Applications*, 2015, Vol. 5, pp.160-170.

[28]. Mirabedini, S.M., Mohseni, M., PazokiFard, S., Esfandeh, M. Effect of tio2 on the mechanical and adhesion properties of rtv silicone elastomer coatings. *Colloids and Surfaces A: Physicochemical and Engineering Aspects* 2008, *317*, 80-86.

[29]. Lu, C., Cui, Z., Li, Z., Yang, B., Shen, J. High refractive index thin films of zns/polythiourethane nanocomposites. *Journal of Materials Chemistry* 2003, *13*, 526-530.

[30]. Ammala, A., Hill, A.J., Meakin, P., Pas, S.J., Turney, T.W. Degradation studies of polyolefins incorporating transparent nanoparticulate zinc oxide uv stabilizers. *Journal of Nanoparticle Research* 2002, *4*, 167-174.

[31]. Katangur, P., Patra, P.K., Warner, S.B. Nanostructured ultraviolet resistant polymer coatings. *Polymer Degradation and Stability* 2006, *91*, 2437-2442.

[32]. Jalili, M.M., Moradian, S. Deterministic performance parameters for an automotive polyurethane clearcoat loaded with

hydrophilic or hydrophobic nano-silica. *Progress in Organic Coatings* 2009, *66*, 359-366.

[33]. Allen, N.S., Edge, M., Ortega, A., Sandoval, G., Liauw, C.M., Verran, J., Stratton, J., McIntyre, R.B. Degradation and stabilisation of polymers and coatings: Nano versus pigmentary titania particles. *Polymer Degradation and Stability* 2004, *85*, 927-946.

[34]. Mirabedini, S.M., Sabzi, M., Zohuriaan-Mehr, J., Atai, M., Behzadnasab, M. Weathering performance of the polyurethane nanocomposite coatings containing silane treated tio2 nanoparticles. *Applied Surface Science* 2011, *257*, 4196-4203.

[35]. Dhoke, S., Mangal Sinha, T., Khanna, A. Effect of nano-al2o3 particles on the corrosion behavior of alkyd based waterborne coatings. *J Coat Technol Res* 2009, *6*, 353-368.

[36]. B, I., TT, S., H, D., J, D., G, T., M, N. Nanotechnology and the cosmetic chemist. *Cosmetics, aerosols and toiletries in Australia*, 2002, *15*, 10-24.

[37]. Wang, Q., Xue, Q., Shen, W., Zhang, J. The friction and wear properties of nanometer zro2-filled polyetheretherketone. *Journal of Applied Polymer Science* 1998, *69*, 135-141.

[38]. Schadler, L.S., Laut, K.O., Smith, R.W., Petrovicova, E. Microstructure and mechanical properties of thermally sprayed silica/nylon nanocomposites. *J Therm Spray Tech* 1997, *6*, 475-485.

[39]. Min Zhi, R., Ming Qiu, Z., Hong, L., Hanmin, Z., Bernd, W., Klaus, F. Microstructure and tribological behavior of polymeric nanocomposites. *Industrial Lubrication and Tribology* 2001, *53*, 72-77.

[40]. Nuraje, N., Khan, S.I., Misak, H., Asmatulu, R. The addition of graphene to polymer coatings for improved weathering. *ISRN Polymer Science* 2013, *2013*, 8.

[41]. Kuila, T., Bose, S., Mishra, A.K., Khanra, P., Kim, N.H., Lee, J.H. Chemical functionalization of graphene and its applications. *Progress in Materials Science* 2012, *57*, 1061-1105.

[42]. Soldano, C., Mahmood, A., Dujardin, E. Production, properties and potential of graphene. *Carbon* 2010, *48*, 2127-2150.

[43]. Chang, C.-H., Huang, T.-C., Peng, C.-W., Yeh, T.-C., Lu, H.-I., Hung, W.-I., Weng, C.-J., Yang, T.-I., Yeh, J.-M. Novel anticorrosion coatings prepared from polyaniline/graphene composites. *Carbon* 2012, *50*, 5044-5051.

[44]. Chang, K.-C., Hsu, M.-H., Lu, H.-I., Lai, M.-C., Liu, P.-J., Hsu, C.-H., Ji, W.-F., Chuang, T.-L., Wei, Y., Yeh, J.-M., *et al.* Room-temperature cured hydrophobic epoxy/graphene composites as corrosion inhibitor for cold-rolled steel. *Carbon* 2014, *66*, 144-153.

[45]. Asmatulu, R., Ceylan, M., Nuraje, N. Study of superhydrophobic electrospun nanocomposite fibers for energy systems. *Langmuir* 2010, *27*, 504-507.

[46]. Li, B., Olson, E., Perugini, A., Zhong, W.-H. Simultaneous enhancements in damping and static dissipation capability of polyetherimide composites with organosilane surface modified graphene nanoplatelets. *Polymer* 2011, *52*, 5606-5614.

[47]. Asmatulu, R., Mahmud, G.A., Hille, C., Misak, H.E. Effects of uv degradation on surface hydrophobicity, crack, and thickness of mwcnt-based nanocomposite coatings. *Progress in Organic Coatings* 2011, *72*, 553-561.

[48]. Asmatulu, R., Khan, I.S., and Jenkinson, M.L. Improving the corrosion resistances via graphene nanocomposites. In *Size-dependent properties*, M. Aliofkhazaei, N.A., W.I. Milne, C.S. Ozkan, S. Mitura, and J. Gervasoni, Ed. CRC Press / Taylor and Francis Group, LLC.: 2015; pp 465-476.

[49]. Daouda Diouf, “Investigating the Effects of Silanized Graphene Nanocomposite Coatings on Fiber Reinforced Composites Exposed to UV Light and Salt Fog Environments,” M.S. Thesis, Wichita State University, February, 2014.